Preprints of the 21st IFAC World Congress (Virtual)
Berlin, Germany, July 12-17, 2020

Core Temperature Observer Design and Model Parameter Uncertainty Analysis for a Lithium Battery

Dirk Nissing; Himani Suresh Birnale

Faculty of Technology and Bionics, Rhine-Waal University of Applied Sciences, Kleve, Germany
(Tel: +49 2821 80673 636 e-mail: dirk.nissing@hochschule-rhein-waal.de).

Abstract: Temperature monitoring for Lithium ion batteries is an important factor for its properties. Since the core temperature is difficult to measure, a thermal model is used for estimation. In this paper, an offline parameter identification procedure is applied, by which the parameters of a three state lumped thermal model can be identified. Based on the model a Luenberger observer is designed with the strength of compensating variations of the model parameters. Only the easily accessible and measurable temperature of the copper pole is fed back to the observer. The paper deals with the robustness analysis of the proposed observer in that the actual plant differs from the model considered in the observer. The capability of the approach is beneficial as an online (and computational power consuming) parameter identification is no longer required. Instead, the thermal model is obtained offline and the observer is robust against model parameter variations, e. g. ageing, so that a continuous update of the model is not required.

Keywords: Observers, Identification, Temperature measurement, Energy storage, Uncertainty, State space methods.

1. INTRODUCTION

Lithium ion batteries are widely used as energy storage devices for mobile applications; in particular in the last several years battery driven electric vehicles have been increased significantly and are still growing (Pistoia, 2009). It has been shown that the temperature of the battery is important for their performance, efficiency, safety, and capacity (Waldmann et al, 2014). Battery management systems (BMS) take into account the battery temperature, although the core temperature of the battery derives the above mentioned properties and it is difficult to measure directly (Lin et al, 2012), (Zhang et al, 2019). Due to that difficulty the temperature is often measured on or near the poles of the cell.

Owing to their narrow operating temperature range, an accurate prediction of the battery temperature is absolutely essential so as to maintain the longevity, performance and safety of these batteries. Studies (Forgez et al, 2010) have shown that, under typical conditions (such as a HEV drive cycle), the cells may experience a temperature difference between the core and the surface of 10°C or more. The BMS typically use thermal models to predict the core temperature and adapt the current flow accordingly so that the efficiency of a battery is at its optimum.

The contribution of the paper lays is the development of an effective temperature observer, so that less computational power is needed for the BMS. The computational power consuming identification process for the thermal model (Lin et al, 2013) is obtained offline, followed by an observer design which is robust against model parameter variations, so that a continuous update of the model is not required.

This paper deals with the design of a robust Luenberger observer in order to predict the core temperature of the battery. The observer is designed for the system states generation; because the observer uses real system output measurements and adjusts its response according to it, a better convergence and a robust observation is expected, even when the parameters of the thermal model are not exact, vary over time or disturbances are added to the system. The designed observer can be used in the BMS to monitor also the health condition of the battery during operation.

The paper is structured as follows: The simplified lumped thermal model in state-space form and the parameter identification is described in Sec. 2, followed by the explanation of the Luenberger observer design in Sec. 3. Sec. 4 shows the temperature observer results including a robustness investigation, where model parameter uncertainties are studied with respect to the observed core temperature.

2. THERMAL MODEL AND PARAMETER IDENTIFICATION OF A LITHIUM ION BATTERY

In order to decide the appropriate battery model to be used, observations were made considering the heat conduction inside the core and poles. According to Nissing, Mahanta, van Sterkenburg (2017) the Biot-number has been determined as 0.14 which justifies assuming a lumped thermal model.

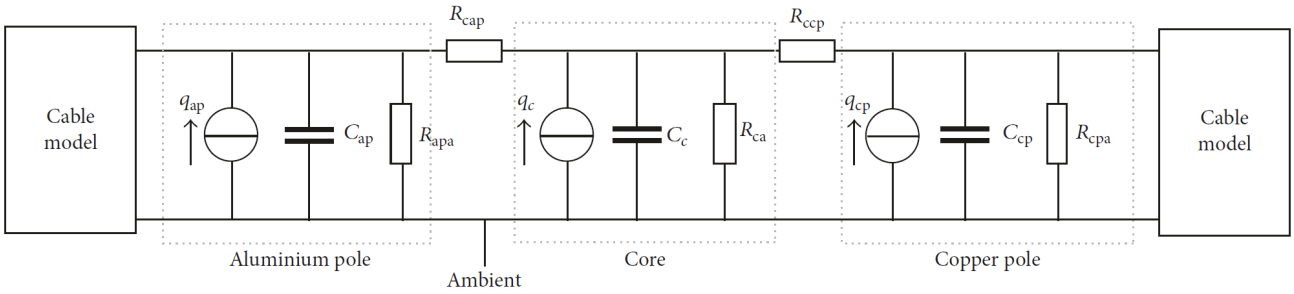

Fig. 1. Thermal RC-network model of cell.

2.1 Lumped Thermal Model

For this study, the simplified lumped thermal model considered is constructed based on first principles, which incorporates the physics of the various processes occurring in the cell. A 100 [A·h] prismatic Lithium Iron Phosphate cell of Sinopoly (LEP100AHA) (van Sterkenburg et al, 2013) was considered for this study. As for prismatic cells, the temperature is often measured at the battery poles; a 1D model is used so as to describe the difference between the temperature at the battery poles and the core. The poles consist of a solid copper or aluminium block with an attached cylindrical top for connecting a current cable. The cell construction also implies two Electric contact resistances (ECR) at each pole (van Sterkenburg and Veenhuizen, 2015), the ECR from cable to pole and the ECR from pole to current collector sheets. Fig. 1 gives the thermal RC representation of the cell model.

The mathematical model of the system is developed by formulating the differential equations with the help of basic physical laws. The thermal model considers the heat capacities as the extension of heat added or removed from the system, which causes temperature variations. It can be shown that, for a specific heat capacity C, the change in temperature T resulting from a net heat flow is given by

$$C\frac{\mathrm{d}T}{\mathrm{d}t} = Q_{\mathrm{net}} \tag{1}$$

where Q_{net} is the net heat flow into or out of the system.

The total heat dissipated at the copper pole, aluminium pole and the core is formulated through

$$C_{\mathrm{cp}}\frac{\mathrm{d}T_{\mathrm{Cu}}}{\mathrm{d}t} = \left(\frac{T_{\mathrm{amb}} - T_{\mathrm{Cu}}}{R_{\mathrm{thcable}}}\right) + \left(\frac{T_{\mathrm{core}} - T_{\mathrm{Cu}}}{R_{\mathrm{ccp}}}\right) + q_{\mathrm{cp}} \tag{2}$$

$$C_{\mathrm{ap}}\frac{\mathrm{d}T_{\mathrm{Al}}}{\mathrm{d}t} = \left(\frac{T_{\mathrm{amb}} - T_{\mathrm{Al}}}{R_{\mathrm{thcable}}}\right) + \left(\frac{T_{\mathrm{core}} - T_{\mathrm{Al}}}{R_{\mathrm{cap}}}\right) + q_{\mathrm{ap}} \tag{3}$$

and

$$C_{\mathrm{c}}\frac{\mathrm{d}T_{\mathrm{core}}}{\mathrm{d}t} = \left(\frac{T_{\mathrm{amb}} - T_{\mathrm{core}}}{R_{\mathrm{ca}}}\right) - \left(\frac{T_{\mathrm{core}} - T_{\mathrm{Cu}}}{R_{\mathrm{ccp}}}\right) - \left(\frac{T_{core} - T_{Al}}{R_{cap}}\right) + q_{\mathrm{c}} \tag{4}$$

with C_{c} the heat capacity of the core, C_{ap} the heat capacity of aluminium pole, C_{cp} the heat capacity of the copper pole, R_{thcable} the thermal resistance of the connector cable, R_{ccp} the thermal resistance from core to copper pole, R_{ca} the thermal resistance from core to ambient, R_{cap} the thermal resistance from core to aluminium, q_{cp} heat dissipated at the copper pole, q_{ap} heat dissipated at the aluminium pole, and q_{c} heat dissipated at the cell core.

The heat dissipations are dependent on the charge/discharge current and the corresponding contact resistances ECR_{Al} and ECR_{Cu} (Pistoia, 2009).

2.2 Parameter Identification

As it is difficult to determine the thermals resistances and the heat capacities experimentally or empirically, a least-square (LS) parameter identification method is applied to determine the parameters of the thermal model, based on input/output measurements (Nissing, Mahanta and van Sterkenburg, 2017). The load current of the battery represents the input while the temperatures at the poles represent the outputs of the measurement. Two sets of measurement have been taken for the parameter identification, in that a constant load as well as the dynamic behaviour is considered for the stimulus. The model parameters are optimized in that the sum of the error $e^2(k)$ between the real process and the model becomes a minimum, (Isermann and Münchhof, 2011).

In order to apply a parameter identification approach, the model fulfils the requirements of (1) stability, (2) controllability, and (3) observability.

The properties of controllability and observability can be proved by use of the Kalman criteria (Isermann and Münchhof, 2011).

The model is validated using a third independent measurement set with 150 [A] maximum current input and the results obtained were satisfactory in terms of the obtained curve fit (Fig. 2). The obtained parameters are listed in Tab 1.

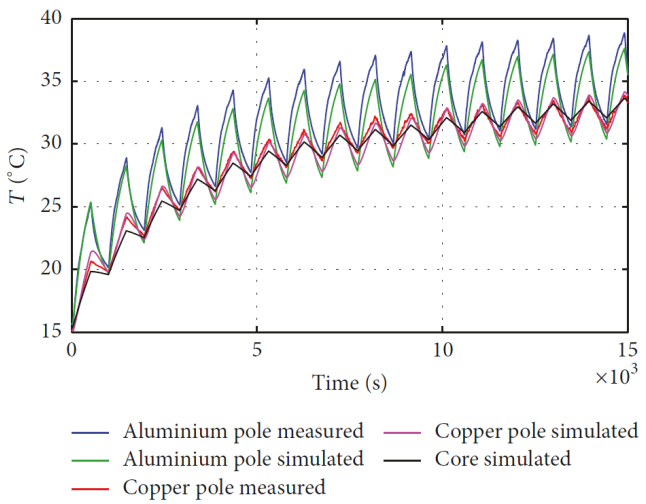

Fig. 2. Validation measurements and comparison.

Table 1. Obtained parameter values

Parameter	Parameter identification
C_{ap} [J·K^{-1}]	52.997
C_c [J·K^{-1}]	3080.2
C_{cp} [J·K^{-1}]	84.792
R_{ca} [K·W^{-1}]	1.3731
R_{cap} [K·W^{-1}]	3.5244
R_{ccp} [K·W^{-1}]	3.1336
ECR_{Al} [μΩ]	73.786
ECR_{Cu} [μΩ]	22.207

2.3 State-Space Model

In order to design a model based observer, the thermal model of the battery has to be transformed into a state-space model.

$$\begin{aligned} \dot{x} &= A\,x + B\,u \\ y &= C\,x + D\,u \end{aligned} \tag{5}$$

With the introduction of the state vector

$$x = \left[T_{\mathrm{Cu}} \quad T_{\mathrm{Al}} \quad T_{\mathrm{core}}\right]^{\mathrm{T}} \tag{6}$$

and the input vector

$$u = \left[T_{\mathrm{amb}} \quad q_{\mathrm{cp}} \quad q_{\mathrm{ap}} \quad q_{\mathrm{c}}\right]^{\mathrm{T}} \tag{7}$$

it yields the system matrix

$$A = \begin{bmatrix} \frac{-1}{C_{\mathrm{cp}}}\left(\frac{1}{R_{\mathrm{thcable}}}+\frac{1}{R_{\mathrm{ccp}}}\right) & 0 & \frac{1}{C_{\mathrm{cp}}R_{\mathrm{ccp}}} \\ 0 & \frac{-1}{C_{\mathrm{ap}}}\left(\frac{1}{R_{\mathrm{thcable}}}+\frac{1}{R_{\mathrm{cap}}}\right) & \frac{1}{C_{\mathrm{ap}}R_{\mathrm{cap}}} \\ \frac{1}{C_{\mathrm{c}}R_{\mathrm{ccp}}} & \frac{1}{C_{\mathrm{c}}R_{\mathrm{cap}}} & \frac{-1}{C_{\mathrm{c}}}\left(\frac{1}{R_{\mathrm{ca}}}+\frac{1}{R_{\mathrm{ccp}}}+\frac{1}{R_{\mathrm{cap}}}\right) \end{bmatrix} \tag{8}$$

and the input matrix

$$B = \begin{bmatrix} \left(\frac{1}{R_{\mathrm{thcable}}}+\frac{1}{C_{\mathrm{cp}}}\right) & \frac{1}{C_{\mathrm{cp}}} & 0 & 0 \\ \left(\frac{1}{R_{\mathrm{thcable}}}+\frac{1}{C_{\mathrm{ap}}}\right) & 0 & \frac{1}{C_{\mathrm{ap}}} & 0 \\ \left(\frac{1}{R_{\mathrm{thcable}}}+\frac{1}{C_{\mathrm{c}}}\right) & 0 & 0 & \frac{1}{C_{\mathrm{c}}} \end{bmatrix} \tag{9}$$

For the observer feedback it is considered, that the temperature at the copper pole T_{Cu} can be easily measured, thus

$$C = \begin{bmatrix}1 & 0 & 0\end{bmatrix}, D = \begin{bmatrix}0 & 0 & 0 & 0\end{bmatrix}. \tag{10}$$

3. OBSERVER DESIGN

The observer design starts with the selection of type of observer depending upon the system requirements and availability of states. Various types of observer techniques can be seen such as open loop state, functional observers, sliding mode, adaptive, proportional – integral, or reduced order observers etc. (Ellis, 2002).

The closed loop Luenberger observer design is used in this paper, because of its advantage that it takes into consideration the output of the plant and adjusts the observer output according to the variations in the plant (Luenberger, 1971). The feedback loop also enables the placement of the poles to desired locations in order to achieve the required dynamics (Nise, 2011), (Dorf and Bishop, 2010). The full order observer design can be used to compare all the observed states with actual readings for validation.

A closed loop Luenberger observer for the system given in Sec. 2.3 is represented in state format

$$\begin{aligned} \dot{\hat{x}} &= A\,\hat{x} + B\,u + L\left(y - \hat{y}\right) \\ \hat{y} &= C\,\hat{x} + D\,u \end{aligned} \tag{11}$$

where $(\hat{*})$ denotes the predicted variable/state. The observer model uses the same system matrix as the plant model and the difference between measured and observed output is multiplied by the observer gain L and is fed back to reduce the error. The estimation error e_{x} present in the observed states is given as,

$$e_{\mathrm{x}} = x - \hat{x}. \tag{12}$$

Differentiation of the estimation error (12) with respect to time gives the equation for the observer error dynamics

$$\dot{e}_{\mathrm{x}} = \left(A - L\,C\right)e_{\mathrm{x}}. \tag{13}$$

Fig. 3 shows the block diagram of the closed loop Luenberger observer where double lines represent vector signal whereas a single line shows a scalar signal.

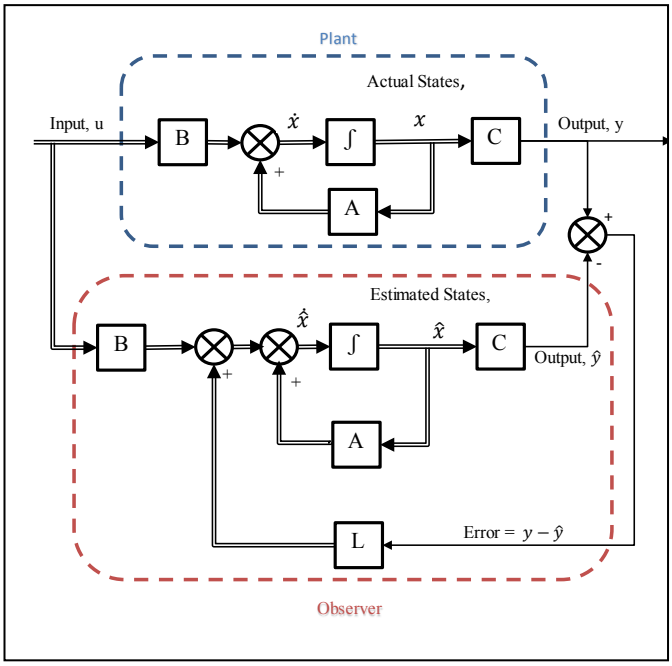

Fig. 3. Block diagram of closed loop observer.

The plant system initially needs to be checked for its observability, before an observer is designed. With the help of Kalman criteria (Isermann and Münchhof, 2011) the observability matrix is found to be full rank, which indicates that the system under consideration is completely observable and the observer can be parameterized by the pole placement method. The desired poles are chosen, so that an acceptable dynamic behaviour is achieved and the observer is still not sensitive against measurement noise.

4. TEMPERATURE OBSERVATION RESULTS AND MODEL UNCERTAINTY INVESTIGATION

The observed temperatures by the designed observer need to be verified with the actual battery temperatures to analyse the correctness. Fig. 4 and 5 show the observed temperatures and the measured copper pole temperature over time, where Fig. 4 represents a static battery loading and Fig. 5 shows a dynamic loading cycle. It is evident from the graphs that the observed copper pole temperature converges to the copper pole temperature measured on the actual battery. Further, in this section the observer performance output is checked for various parametric deviations.

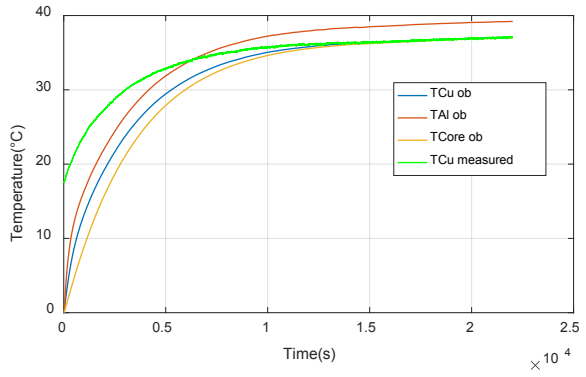

Fig. 4. Observed states under steady loading condition.

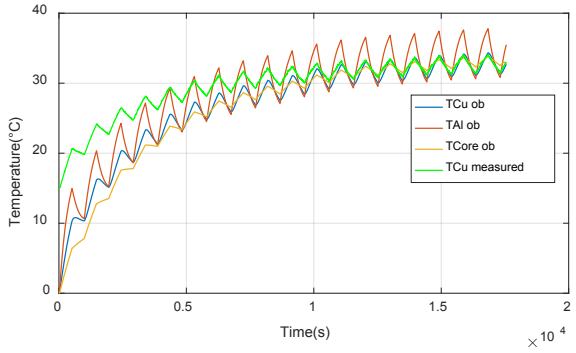

Fig. 5. Observed states under dynamic loading condition.

4.1 Verification of Robustness

The designed observer should maintain its performance and stability even when the model considered for the observer design is no longer accurate. This ability is called as the robustness of the system/observer and investigates the effect to model parameter uncertainties. A robust observer is capable of compensating the disturbances and give acceptable state variable values. The actual plant properties may vary due to different reasons and can introduce inaccuracies in the observer model.

4.2 Model Inaccuracies

Two types of inaccuracies can be found in a model considered for the observer design.

Firstly, the inaccuracies introduced to an observer model due to the faults present in the plant model introduced during the parameter identification or system modelling phase. This type of error is seen for very complex plants or highly nonlinear behaviour because they are often difficult to model accurately with a set of linear differential equations. The output results of the plant model under consideration are compared with the measurements taken on the actual battery, which shows deviations of less than 1% under steady loading condition and also overall dimensional correctness for dynamic loading condition (Nissing, Mahanta and van Sterkenburg, 2017). This indicates that the plant model under consideration is correct with acceptable output.

Second type of inaccuracy is introduced due to deviations in parameters of the actual plant during operation. This deviation in parameters may be caused due to aging of the electric battery components or replacement of any battery component without changing the observer model. It is seen that the parameter values of electric components vary by up to ±20 % (Ellis, 2002).

4.3 Model Parameter Variation

The variations in the plant model are simulated with the help of a variation factor *v*. The plant model parameters mentioned in Tab. 1 and the connecting cable parameters are multiplied by the variation factor to simulate the percentage variation in

the actual plant. Thus the considered system matrix $\widetilde{A}$ and the input matrix $\widetilde{B}$ of the plant model change after multiplication by the variation factor, whereas the respective matrices of the observer model remain unchanged. The main objective of the simulation is to examine the effect of parametric variation on the observed poles and core temperature values.

4.4 Results

The various parametric changes and loading conditions are analysed in a simulation where the temperature profiles of the plant temperatures and the observed temperatures are studied for different parametric changes.

Two measurement sets are considered in this investigation: Measurement set 1 considers a steady loading while measurement set 2 takes into account a dynamic loading condition. For the measurement set 1 the results are exemplarily shown in Fig 6, where the observed temperatures are plotted as a function of time taking into account a parameter change of 0 %, +20 %, and -20 % for each temperature. The results with 0 % parameter change are considered as ideal and the corresponding error-plots show the temperature deviation against that reference.

Fig. 7 and Fig 8 illustrate the relation between the average percentage error in the observed states with respect to the percentage change in the battery parameters under steady and dynamic loading condition respectively. It is evident from the graph that the average percentage error for the pole and core temperatures increases with different gradients per increase in the amount of parametric change. The error at the copper pole increases at smaller gradient.

It can be seen from both loading conditions that the observer shows a robust behaviour. The observed core temperature of the battery contains an average percentage error less than 3 % even under ±20 % parameter change for both loading conditions.

The observed temperature of the aluminium pole shows higher error values and more fluctuations without any definite pattern. This behaviour can be explained as the ECR of the aluminium pole is measured to be 4 times the ECR of the copper pole (van Sterkenburg and Veenhuizen, 2015). Also the specific resistance of the aluminium is 50 % higher than that of the copper. Hence, as compared to the copper pole, the aluminium pole model can respond differently to the same heat dissipation stimuli. But the main reason is that the actual copper pole temperature is fed back to the observer and this error is minimized even under the presence of parametric variations.

It is also seen in the simulation that the error is high during initial time and gradually converges to the steady state value or pattern. The fluctuations were observed in the estimation error response under dynamic loading condition. Furthermore, the convergence time of the observed states is not affected by the variations in the plant model.

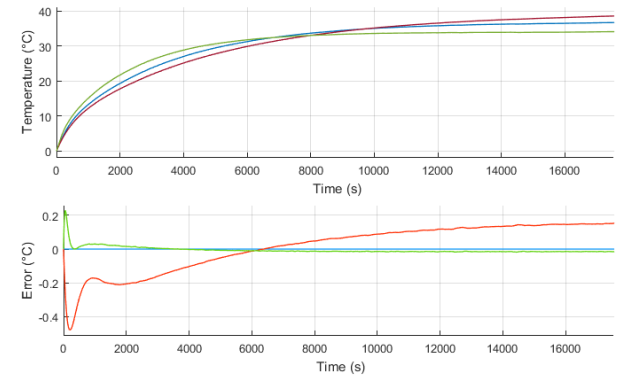

(a) Observed Copper pole temperature

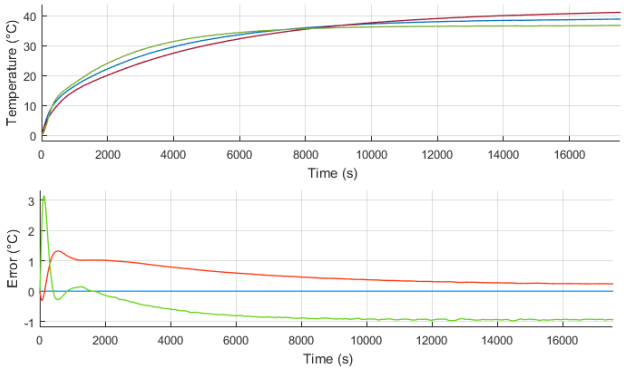

(b) Observed Aluminum pole temperature

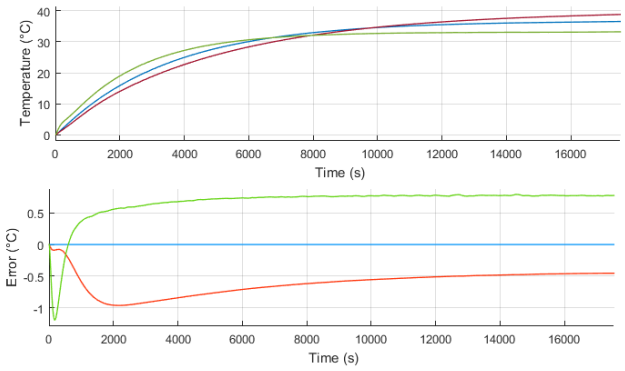

(c) Observed Core temperature

Fig. 6. Observer response with parametric deviation under steady loading.

5. CONCLUSION, SUMMARY AND OUTLOOK

The core temperature of a Lithium battery cell is important for its performance, efficiency, safety, and capacity and is influenced by the environmental temperature and by the charging and discharging process itself. BMS take into

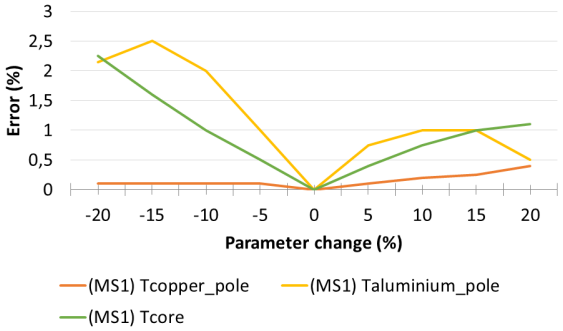

Fig. 7. Observation error vs. parametric change under steady loading condition.

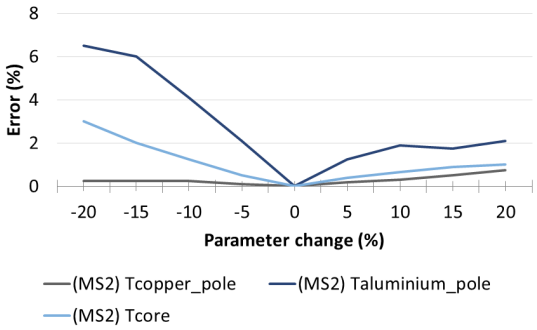

Fig. 8. Observation error vs. parametric change under under dynamic loading condition.

account this effect although the core temperature is usually not measurable. The core temperature can be estimated by a three state thermal model which results in the determination of the model parameters, which can be realized by a parameter identification scheme based on a least square algorithm. In this paper, a Luenberger observer design is proposed and applied, because of its advantage considering and compensating variations of the model parameters. In order to predict all the states, only the easily accessible, measurable copper pole temperature with comparatively less error and fluctuations is fed back to the observer. The temperature observer shows the capability to predict the core temperature even when the model considered in the observer deviates from the behaviour of the actual plant. Simulation studies show a core temperature error of <3 % even for a parameter change of ±20 %. The methodology developed in this paper has been verified with simulations and it is to be validated with experiments in the future.

The strength of the presented approach lays in effectiveness so that less computational power is needed for the BMS. The computational power consuming identification process for the thermal model (Lin et al, 2013) is obtained offline and it has been shown that the observer is robust against model parameter variations, so that a continuous update of the model is not required.

High power applications, such as BEV or HEV, usually have multiple battery cells in series to meet the high power and energy requirements. Thus, a future scope considers the extension of the given approach on a single cell to a battery with multiple cells. Therefore the thermal model of the battery has to be extended and temperature interactions between the cells have to be considered.

REFERENCES

Dorf, R. C., and Bishop, R. H. (2010). *Modern Control Systems*. 12th rev. Edition, Prentice Hall, Upper Saddle River, NJ.

Ellis, G. (2002). *Observers in Control Systems: A Practical Guide*. Elsevier.

Forgez, C., Vinh Do, D., Friedrich, G., Morcrette, M., and Delacourt, C. (2010). Thermal modeling of a cylindrical LiFePO4/graphite lithium-ion battery. Journal of Power Sources, vol. 195, no. 9, pp. 2961–2968.

Isermann, R., and Münchhof, M. (2011). *Identification of Dynamic Systems*. Springer, Berlin, Germany.

Lin, X., Perez, H.E., Siegel, J.B., Stefanopoulou, A.G., Li, Y., Anderson, R.D., Ding Y., and Castanier M.P. (2013). Online Parameterization of Lumped Thermal Dynamics in Cylindrical Lithium Ion Batteries for Core Temperature Estimation and Health Monitoring. *IEEE Transactions on Control Systems Technology*, Vol. 21, No. 5.

Lin, X., Stefanopoulou, A.G., Perez, H.E., Siegel, J.B., Li, Y., and Anderson, R.D. (2012). Quadruple Adaptive Observer of the Core Temperature in Cylindrical Li-ion Batteries and their Health Monitoring. *IEEE American Control Conference*, pp.578-583.

Luenberger, D. (1971). An introduction to observers. *IEEE Trans. Autom. Control*, vol. 16, no. 6, pp. 596–602.

Nise, N. S. (2011). *Control Systems Engineering*. 6th ed. Wiley.

Nissing, D., Mahanta, A., and van Sterkenburg, S. (2017). Thermal Model Parameter Identification of a Lithium Battery. *Journal of Control Science and Engineering*, Volume 2017, Article ID 9543781, 8 pages. doi:10.1155/2017/9543781

Pistoia, G. (2009). Battery Operated Devices and Systems. Elsevier, Oxford, UK.

van Sterkenburg, S., and Veenhuizen, B. (2015). The modelling of the temperature at the poles and core of a large prismatic LiFePO4 cells. *Proceedings of the European Battery, Hybrid and Fuel Cell Electric Vehicle Congress*, Brussels, Belgium.

van Sterkenburg, S., Fleuren, T., Veenhuizen, B., and Groenewegen, J. (2013). Design and test of a battery pack simulator. *Proceedings of the EVS27 International Battery, Hybrid and Fuel Cell Electric Vehicle Symposium*, IEEE, Barcelona, Spain.

Waldmann, T., Wilka, M., Kasper, M., Fleischhammer, M., and Wohlfahrt-Mehrens, M. (2014). Temperature dependent ageing mechanisms in Lithium-ion batteries - a Post-Mortem study. Journal of Power Sources, vol. 262, pp. 129–135.

Zhang, D., Dey, S., Perez, H.E., Moura, S.J. (2019). Real-Time Capacity Estimation of Lithium-Ion Batteries Utilizing Thermal Dynamics. *IEEE Transactions on Control Systems Technology*, January 2019.